Infrared Spectrum of *p*-Hydrogen Crystals Ionized by 3 MeV Electrons: Cluster Ions of Hydrogen in Condensed Phase†

Man-Chor Chan,‡ Mitchio Okumura,§ and T. Oka*

Department of Chemistry and Department of Astronomy and Astrophysics, The Enrico Fermi Institute, The University of Chicago, Chicago, Illinois 60637-1403

Received: November 3, 1999

High purity *p*-H_2 crystals have been ionized by 3 MeV electron beams from a van de Graaff accelerator, and their infrared spectra have been studied from 1800 to 8000 cm^{-1} using a Fourier transform infrared spectrometer. Out of 16 spectral lines induced by the electron bombardment, 5 lines have been assigned to *p*-H_2 spectral lines that are induced by the electric field of charges deposited in the ionized crystal. The stability of such spectral lines several hours after electron bombardment demonstrates the stability of charges in the crystal. A mechanism of stabilization of positive and negative charges as cation clusters $H_3^+(H_2)_n$ and anion clusters $H^-(H_2)_n$, respectively, is proposed.

Introduction

The *p*-hydrogen crystal is unique as a sample of solid-state spectroscopy. Because of the very weak and highly symmetric intermolecular interactions and the quantum nature of the crystal, we can observe extremely sharp spectral lines with line widths that are smaller than those of Doppler limited gaseous spectra ($\Delta\nu/\nu < 10^{-6}$).[1−3] These special characteristics of the crystal also make it an ideal matrix for high-resolution spectroscopy of species deposited in it as impurities. High-resolution spectra of *o*-H_2,[4] deuterated hydrogen,[5] CH_4,[6] CH_3,[7] carbon clusters,[8,9] and other species[9] have been reported. In this paper, we report our attempt to observe spectra of *p*-H_2 crystals in which electric charges are deposited by 3 MeV electron bombardment.

Infrared spectra of ionized solid hydrogen and its isotopic species have been reported in many papers using ionization by β-ray of tritium,[10−14] bombardment of high-energy proton beams,[15−21] and γ-ray irradiation.[22] Many spectral features have been observed and explained by invoking various physical effects, including Stark shift,[12,20,23,24] electron bubbles,[14,18,19,21] electron trapping,[16−25] interference effect,[17,26] polaron states,[18,27] and cluster ions.[21,28]

Together with our γ-ray experiments published earlier,[22] our approach is different from previous works in that we use highly pure (99.8%) *p*-H_2 crystals. In such a crystal, practically all molecules are in the lowest $J = 0$ rotational level, and the spectrum prior to the ionization is extremely simple. In addition, the 3 MeV electron beam has higher penetrating power than the 15 MeV proton beam both in the hydrogen crystal and in the metal foil enclosing the crystal. Those, together with smaller line widths of spectral lines, allow us to observe the charge-induced spectrum with higher clarity.

Experimental Section

Experiments were conducted at Argonne National Laboratory using 3 MeV electron beams from the van de Graaff accelerator. A Fourier transform infrared spectrometer (BOMEM DA2) with the spectral resolution of 0.02 cm^{-1} and a gas handling system for the preparation of *p*-H_2 crystals were moved to the accelerator site. A schematic diagram of the experimental setup is shown in Figure 1.

An in-line *o*- to *p*-H_2 converter made of a column of APPACHI catalyst was used in the gas handling system to generate *p*-H_2. Nearly pure (∼99.8%) *p*-H_2 gas was generated by passing ultrahigh-purity normal hydrogen gas through the converter maintained at ∼20 K in a liquid H_2 bath. The "impurity" *o*-H_2 concentration was measured from the integrated absorption intensity of the $Q_1(1)$ transition. *p*-H_2 crystals were prepared by pulsing the *p*-H_2 gas at a pressure of 50−100 Torr into a sample cell whose temperature was maintained at ∼10 K. Crystal samples prepared by this method were normally optically transparent with reproducible optical quality. Examination of the samples through crossed polarizers show some mechanical strain but do not show boundaries of polycrystals. Various high-resolution spectroscopic observations have shown that the samples have a hexagonal close-packed crystal structure.[2,3,29]

The sample cell was made of copper with an inner diameter of 2 cm and optical path of 2.5 cm. The cell was sealed with two 1-mm-thick sapphire windows using indium gaskets. As shown in Figure 1, the 3 MeV electron beam was passed through the cell perpendicular to the optical path. For this purpose, the cell had two extra holes sealed by 50-μm-thick Duralmin windows using indium gaskets. After the beam was passed through the cell, the electrons were collected, and their current was measured. The 3 MeV electron was pulsed with a pulse width of ∼5 ns and a repetition rate of ∼30 kHz, and the average current was ∼0.1 μA.

Infrared radiation with the wavenumbers from 1800 to 8000 cm^{-1} generated from a globar source of the BOMEM DA2 FTIR spectrometer was passed through the crystal and detected by an InSb detector, and the signal was Fourier analyzed. Sampling

† Part of the special issue "Marilyn Jacox Festschrift".

‡ Present address: Institute for Astrophysics and Planetary Sciences, Ibaraki University, Mito Ibaraki, Japan 310.

§ Present address: Department of Chemistry, California Institute of Technology, Pasadena, CA 91125.

* To whom correspondence should be addressed. E-mail: t-oka@uchicago.edu.

10.1021/jp993890h CCC: $19.00
Published on Web 03/17/2000

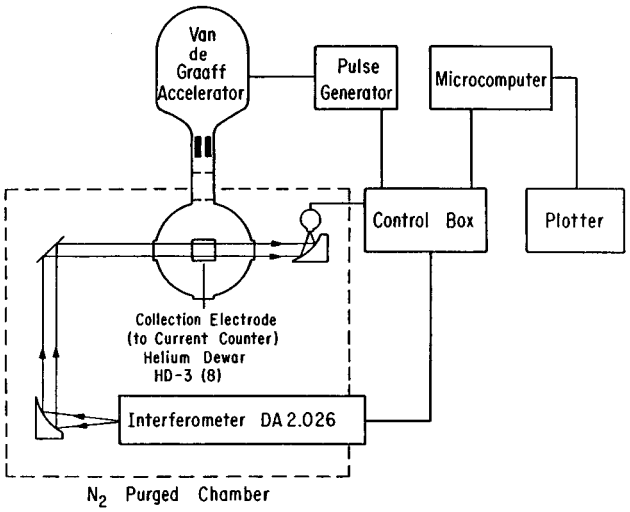

Figure 1. Block diagram of the experimental setup. The 3 MeV electron beam and the infrared beam are perpendicular to each other. The electron beam is pulsed at a repetition rate of ~30 kHz with pulse widths of ~5 ns. Sampling of the infrared signal is synchronized to the electron pulse.

of the infrared was synchronized to the pulse of the electron beam to maximize the signal of possible short-lived species. An attempt was made to reduce the atmospheric water absorption by surrounding the optical path with vinyl sheets and blowing nitrogen into it.

Observed Results

We have observed 13 transitions from 2000 to 4200 cm^{-1} in p-H_2 crystals induced by the bombardment of 3 MeV electrons. We also observed a broad near-infrared absorption that had a lifetime on the order of 1 s. This absorption is similar in wavenumber region, line width, and lifetime as the absorption reported by Poll et al.[30] in solid D_2 and H_2 containing tritium and by Selen et al.[16] in proton-irradiated solid D_2. The broad absorption was explained by Bose and Poll[25] as due to oscillation of localized electron bubbles. On the other hand, we have not observed the sharp asymmetric "B feature" at 4120 cm^{-1} reported by Brooks et al.[17] and interpreted by Bose and Poll as due to interference between the dipole of the localized electron and the charge-induced dipole moment.[26] Another striking difference between our observations and previous observations was that the 13 induced spectral lines reported here all had very long lifetimes. No sign of intensity decay was observed several hours after the electron beam was turned off, indicating the stability of all the carriers causing the spectral lines.

Three spectral lines induced by electron bombardment in the Q branch region of H_2 are shown in Figure 2 with asterisks. The strongest line at ~4153 cm^{-1} (without an asterisk) is the vibron broadened $Q_1(0)$ transition induced by the quadrupole moment of the $J = 1$ o-H_2 impurity.[34] The sharp line at 4146.56 cm^{-1} is the $Q_1(1)$ transition of the o-H_2 impurity.[34] Out of the three induced lines, the highest at 4149.66 cm^{-1} is very sharp and strong, and its wavenumber agrees with the $\nu = 1 \leftarrow 0$, $J = 0 \leftarrow 0$ $Q_1(0)$ Raman-type transition first measured by Bhatnagar et al.[31] at 4149.81 cm^{-1}. This transition was later measured by stimulated Raman spectroscopy[29] at 4149.75 cm^{-1}. This transition is infrared inactive but becomes strongly infrared active in the ionized p-H_2 crystal because of the electric field due to charges deposited in the crystal through the Condon effect.[32,33] The same transition was observed in our γ-ray irradiated p-H_2 crystals.[22] As discussed in the paper,[22] this

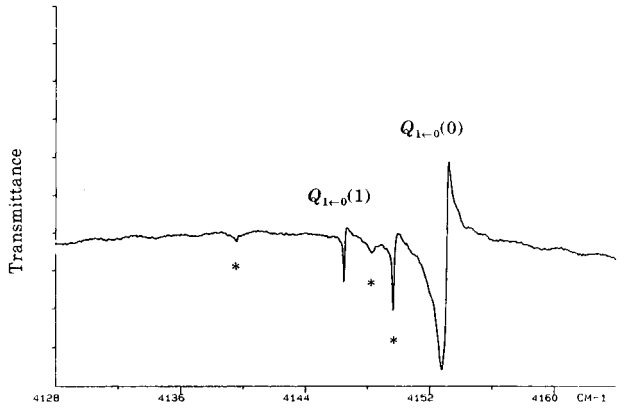

Figure 2. FTIR spectrum of the ionized p-H_2 crystal at 0.1 cm^{-1} resolution in the 2.4 μm Q branch region. Charge-induced transitions are marked with asterisks. The sharp transition at 4149.66 cm^{-1} is accompanied by two broader lines at 4139.54 and 4148.24 cm^{-1}. Asymmetry of the signals is an artifact created by the scanning mechanism of the spectrometer.

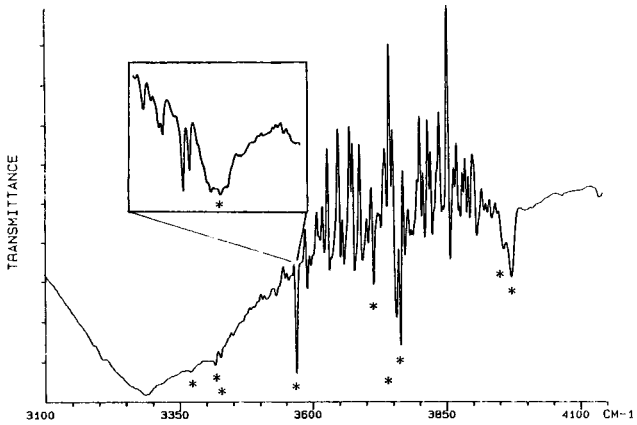

Figure 3. FTIR spectrum of the ionized p-H_2 crystal at 4 cm^{-1} resolution in the 2.7 μm H_2O spectral region. Charge-induced transitions are marked with asterisks. The two lines at ~3965 cm^{-1} are assigned to the Stark shifted $Q_1(0)$ transitions of H_2 which are the closest to charges H_3^+ and H^-. The three lines at ~3750 cm^{-1} are due to H_2O, the isolated line at ~3570 cm^{-1} is due to OH, and the three lines at ~3400 cm^{-1} are due to NH_3.

transition is caused by a macroscopic electric field (on the order of 10 kV/cm) in the crystal due to the imbalance of positive and negative charges. The absorption is caused by many body radiative interactions, and the vibron momentum selection rule[34] $\Delta k = 0$ is obeyed, leading to the very sharp spectral line.

The other two induced spectral lines in Figure 2 at 4148.28 and 4139.54 cm^{-1} are broader and have line widths of ~1 cm^{-1}. They are assigned to the $Q_1(0)$ field induced transitions of p-H_2 near the deposited charges but not at the nearest neighbor. Unlike the 4149.66 cm^{-1} line discussed, these lines are red Stark shifted from the field free position due to the large Coulomb field of neighboring charges. The p-H_2 molecules causing these lines are much fewer than those causing the 4149.66 cm^{-1} line, but they get their intensity from the large local field (on the order of 100 MV/cm) since the intensity of absorption induced by the Condon effect is proportional to the square of the electric field. The absorption is caused by individual molecules, and the vibrons are localized.

A group of nine induced spectral lines observed in the 2.7 μm region are shown by asterisks in Figure 3. The instrument resolution was 4 cm^{-1}. The complicated features at the center that dominate the spectrum are inevitable atmospheric water absorption. Out of the nine induced lines, the two broad lines

TABLE 1: Observed Spectral Lines in Ionized *p*-H_2 Crystals[a]

wavenumber (cm^{-1})	assignment
4149.660[b]	$Q_1(0)$ transition with the vibron momentum selector rule $\Delta k = 0$ induced by the macroscopic electric field in the crystal
4148.24, 4139.54 [c]	Stark shifted $Q_1(0)$ transitions induced by strong local Coulomb charges; they are due to the H_2 molecules close to, but not at, the nearest neighbor of the charges
3970.7, 3957.2	Stark shifted $Q_1(0)$ transitions due to H_2 at the nearest neighbor of charges
3764.4, 3756.7, 3711.7	H_2O
3569.1	OH^-
3426.9, 3417.2, 3371.0	NH_3
2109.7	H_3^+ in $H_3^+(H_2)_n$?

[a] The spectrum was recorded with a resolution of 4 cm^{-1} unless otherwise noted. [b] Resolution of 0.02 cm^{-1}. [c] Resolution of 0.1 cm^{-1}.

at 3957.2 and 3970.7 cm^{-1} are assigned to the stretch vibration of *p*-H_2 at the nearest neighbor position of the charges. Such H_2 molecules are part of ion clusters, and their absorption has been measured in the gas phase by Okumura et al[35,36] at 3910 for H_5^+, 3980 for H_7^+, and 4020 cm^{-1} for H_9^+. The symmetric breathing vibration of H_3^+ at the center of the cation clusters was observed by Okumura et al. at 3532 cm^{-1} for H_5^+, but it was too weak to observe for H_7^+, and it is infrared inactive in H_9^+ or in *p*-H_2 crystals. It is tempting to assign the two broad lines to cation clusters and anion clusters, but more evidence is needed for confirmation.

The other seven induced lines in Figure 3 are most likely due to oxygen and nitrogen impurities. Minimal mixing of air in the gas-handling system and desorption of air from metal windows due to electron bombardment cause these lines because of the strong spectral intensities of O−H and N−H stretching vibrations. The three induced lines around 3750 cm^{-1} are assigned to the H_2O ν_3-band based on agreement with previous work;[37a] the transitions at 3764.4 ($2_{02} \leftarrow 1_{01}$), 3756.7 ($1_{01} \leftarrow 0_{00}$), and 3711.7 cm^{-1} ($0_{00} \leftarrow 1_{01}$) all start from the lowest two water rotational levels. The strong isolated line at 3569.1 cm^{-1} is assigned to the OH^- anion based on the observation of Suzer and Andrews.[37b] The three lines at around 3400 cm^{-1} are assigned to NH_3.[38] The intensities of the O−H and N−H stretching vibrations differ from crystal to crystal.

In the lower wavenumber region, three lines were observed that are clearly due to impurities: CO_2 (2340.2 cm^{-1}), N_2O (2232.1 cm^{-1}), and CO (2136.1 cm^{-1}). They are most likely due to the gaseous molecules frozen outside the sample cell sapphire windows. Their intensities vary depending on conditions, and under the optimum conditions, they are invisible. A very weak line was observed at 2109.7 cm^{-1}. It is tempting to assign this line to H_3^+ at the core of cation clusters based on agreement of its line position with theoretical values obtained by using certain basis sets,[39,40] but this has to be confirmed both experimentally and theoretically. Observed spectral lines are listed in Table 1.

Formation of Ionic Clusters

On the basis of the observed induced spectrum and knowledge acquired from various plasma chemical experiments,[41] we speculate that the processes shown in Figure 4 occur, that is,

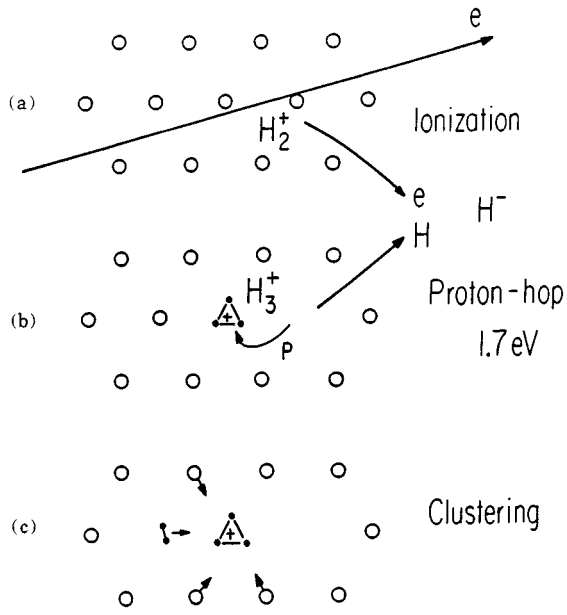

Figure 4. Proposed sequence of events: (a) Ionization of H_2 by an electron. (b) Formation of H_3^+ by proton hopping from H_2^+ to H_2. (c) Formation of ionic clusters $H_3^+(H_2)_n$. Hydrogen atom produced in panel b traps an electron to produce H^-, which also forms ionic clusters $H^-(H_2)_n$.

(a)ionization of H_2 to produce H_2^+; (b) ion-neutral reaction between H_2^+ and H_2 to produce H_3^+ and H; and (c) clustering due to the Langevin force between H_3^+ and neighboring H_2 to produce $H_3^+(H_2)_n$. Some of them are violent processes accompanying generation of large energy and momentum, but the quantum nature of solid hydrogen[42] absorbs them and reproduces nice crystals surrounding the cationic cluster. The fate of negative charges is less certain, but we speculate that the electron produced in (a) is stabilized on atomic hydrogen producing H^- that attracts neighboring H_2 to form anionic clusters of $H^-(H_2)_n$. Each of these processes is discussed.

Ionization (Figure 4a). Using the equation

$$L(E) = -\frac{1}{\rho}\frac{dE(x)}{dx} \tag{1}$$

relating the energy of electrons $E(x)$ after passing a distance of x in the crystal with density ρ and the linear energy transfer function $L(E)$, $E(x)$ can be calculated as

$$E(x) = E(0) - \int_0^x \rho L(E)\, dx \tag{2}$$

Using the values of $L(E)$ listed in Souers' book,[43] $\rho = 0.0434$ mol cm^{-3} and $E(0) = 3$ MeV, we estimate that energy of $E(2.5$ cm$) - E(0) = 0.9$ MeV is lost for each electron in passing through the 2.5 cm of the *p*-H_2 crystal. If we assume that ~30 eV is lost for each ionization of H_2, that is, the ionization potential of 15.4 eV and wasted energy dissipated into the crystal, each electron will produce ~30 000 H_2^+ in its path through the reaction

$$H_2 + e^- \rightarrow H_2^+ + e^- + e^- \tag{3}$$

In many cases, the secondary electrons have very high energy and cause cascade ionizations in the crystal; the number of 30 000 includes all these processes. Since the average current of the 3 MeV electron is ~0.1 μA, we estimate that about 2×10^{16} s^{-1} of H_2^+ and e^- are produced in the crystal. The outcome of these species is discussed below.

In addition to the ionization reaction of eq 3, dissociative ionization

$$H_2 + e^- \rightarrow H + H^+ + e^- + e^- \quad (4)$$

and dissociation

$$H_2 + e^- \rightarrow H + H + e^- \quad (5)$$

occur. In our crude order of magnitude estimate, we neglect reaction 4 since its rate is less than that of reaction 3 and assume that the rate of reaction 5 is equal to that of reaction 3 since their gaseous cross sections are comparable.[44]

Formation of H_3^+ (Figure 4b). The H_2^+ ion produced in reaction 3 immediately reacts with a neighboring *p*-H_2 to produce an H_3^+ ion through the ion-neutral reaction[45,46]

$$H_2^+ + H_2 \rightarrow H_3^+ + H \quad (6)$$

which has the large Langevin cross section[47] of ~100 Å.[2] Because of the large difference in proton affinities of molecular (4.4 eV) and atomic (2.7 eV) hydrogen, this reaction is highly exothermic by 1.7 eV. This excess energy is dissipated mostly as the kinetic energy of the H atom but also partly as the internal energy of H_3^+. The latter is dissipated into the energy of lattice vibrations of the surrounding molecules.

The hydrogen atom ejected in reaction 6 with the kinetic energy on the order of 1 eV flies away from H_3^+ because of the soft quantum nature of the surrounding *p*-H_2 crystal;[7,8] there is no cage effect in solid hydrogen. In its flight in the crystal, the H atom loses its energy after colliding with many H_2 molecules and is eventually localized in an hcp site of the crystal (most likely) substitutionally. Since the atomic hydrogen is stable once localized in the crystal, the irradiated crystal contains a great many hydrogen atoms, and they are expected to act as scavengers of electrons as discussed below. The electron spin resonance of H atoms observed by Miyazaki et al.[48,49] provides direct evidence for the existence of the H atom in ionized *p*-H_2 crystals.

Cluster Formation and Stabilization of H_3^+ (Figure 4c). Most of the H_3^+ produced by reaction 6 are destroyed by dissociative recombination with low energy electrons with the

$$H_3^+ + e^- \rightarrow \begin{cases} H + H + H \\ H_2 + H \end{cases} \quad (7)$$

branching ratio of ~3:1.[50] The electrons generated by reaction 3 lose their energy after colliding with many H_2 molecules and exciting phonons. When they reach equilibrium with the cryogenic temperature, their Onsager radius for the reaction with H_3^+ is extremely large, on the order of micrometer, and reaction 7 occurs with very high efficiency. However, as many H atoms are generated through reactions 5−7 and localized in the crystal, they act as electron scavengers because of the sizable electron affinity (0.75 eV) of H. Therefore, some H_3^+ ions escape dissociative recombination. These H_3^+ ions polarize and attract the surrounding *p*-H_2 by the Langevin force and form cationic clusters of $H_3^+(H_2)_n$. Such a cluster is considerably smaller than a hypothetical aggregate in which the clustering H_2 molecules are placed in the regular hcp structure. For example, the distance between H_3^+ and H_2 in the nearest neighbor site is theoretically calculated[40] to be ~2.2 instead of 3.872 Å. The calculated structure of the free $H_3^+(H_2)_n$ cluster has three H_2 molecules in the plane of H_3^+, whereas there exist six H_2 molecules in the hexagonal plane of the crystal. How they are attracted to the central H_3^+ ion presents an interesting theoretical problem. The H_2 molecules at the next nearest neighbor site are attracted less, and those at the next next nearest neighbor site are attracted even less and so on. This must cause stress in the crystal surrounding the ionic cluster, but recent observations[51] of very sharp spectral lines in γ-ray irradiated crystals indicate that the self-repairing nature of *p*-H_2 crystals produces nice, uniform crystals surrounding the ionic clusters. Once stabilized and localized in this form, the cation cluster $H_3^+(H_2)_n$ stays semipermanently in the crystal.

Anionic Clusters and Stabilization of Negative Charges. While the previously mentioned formation and stabilization of the $H_3^+(H_2)_n$ cationic cluster can be concluded with some confidence, the fate of electrons produced in the ionization reaction 3 is less certain. Formation of electron bubbles in the crystal has been suggested.[14,18,19,21] Recently, formation of H_2^- has been proposed based on the observed hyperfine structure of its ESR spectrum.[52,53] We believe that neither of them are stable for a long time in the crystal. In crystals which contain much oxygen impurity, the electrons are stabilized on OH^-. Otherwise, we speculate that the stabilization of electrons is affected by forming anion clusters $H^-(H_2)_n$ in the following steps.

Although the initial several ionizations after the primary Compton scattering may generate electrons with high energy whose mean free path is on the order of the crystal size, the energy and the mean free path are reduced rapidly in the subsequent cascading processes, which are terminated when the electron energy is less than the ionic potential of H_2, 15.4 eV. The mean free path of such an electron is on the order of 0.1 μm, and it gets smaller as the electron loses its energy into the crystal lattice by exciting phonons. These electrons, however, are not readily localized since H_2 has a negative electron affinity. They wander around in the crystal, and many of them fall into the wall of the container made of copper whose work function is 4.56 eV. This causes an imbalance between the positive and the negative charges, which leads to the macroscopic Gauss field and the sharp $Q_1(0)$ transition at 4149.660 cm^{-1} with the vibron momentum selection rule $\Delta k = 0$.[22]

Many other electrons keep losing their energy and reach cryogenic temperature. Such low energy "swarm" electrons are trapped by the atomic hydrogen that are abundantly produced through reactions 5−7 as discussed. The H^- anion thus produced attracts neighboring H_2 molecules and stabilizes in the form of anion clusters $H^-(H_2)_n$. The binding energy against the dissociation $H^-(H_2)_n \rightarrow H^-(H_2)_{n-1} + H_2$ for $n = 1-6$ is on the order of 0.4−0.2 eV.[54] The energy is not sufficiently high to produce stable $H^-(H_2)_n$ in the gaseous phase but stabilizes the anion in *p*-H_2 crystals. We have recently observed very sharp charge-induced spectral lines in γ-ray ionized *p*-H_2 crystals, which allow us to discuss the effect of cation clusters $H_3^+(H_2)_n$ and the anion clusters $H^-(H_2)_n$ separately.[51]

Acknowledgment. We would like to thank R. H. Lowers and A. D. Trifurnac of the Argonne National Laboratory for arrangement and operation of the van de Graaff accelerator. We are grateful to S. S. Lee, K. Takagi, S. Kurokawa and D. P. Weliky for their assistance during the experiment and to T. Momose for discussions. M.C.C. acknowledges the graduate scholarship from the United College, the Chinese University of Hong Kong. This work was supported by the Air Force Grant No. F49620-94-1-0145 and NSF PHYS-9722691.

References and Notes

(1) Okumura, M.; Chan, M.-C.; Oka, T. *Phys. Rev. Lett.* **1989**, *62*, 32.
(2) Oka, T. *Annu. Rev. Phys. Chem.* **1993**, *44*, 299.
(3) Weliky, D. P.; Byers, T. J.; Kerr, K. E.; Momose, T.; Dickson, R. M.; Oka, T. *Appl. Phys. B* **1994**, *59*, 265.
(4) Zhang, Y.; Byers, T. J.; Chan, M.-C.; Momose, T.; Kerr, K. E.; Weliky, D. P.; Oka, T. *Phys. Rev. B* **1998**, *58*, 218.
(5) Weliky, D. P.; Kerr, K. E.; Byers, T. J.; Zhang, Y.; Momose, T.; Oka, T. *J. Chem. Phys.* **1996**, *105*, 4461.
(6) Momose, T.; Miki, M.; Wakabayashi, T.; Shida, T.; Chan, M.-C.; Lee, S. S.; Oka, T. *J. Chem. Phys.* **1997**, *107*, 7707.
(7) Momose, T.; Miki, M.; Uchida, M.; Shimizu, T.; Yoshizawa, I.; Shida, T. *J. Chem. Phys.* **1995**, *103*, 1400.
(8) Miki, M.; Wakabayashi, T.; Momose, T.; Shida, T. *J. Phys. Chem.* **1996**, *100*, 12135.
(9) Fajardo, M. E.; Tam, S. *J. Chem. Phys.* **1998**, *108*, 4237.
(10) Souers, P. C.; Fearon, D.; Garza, R.; Kelly, E. M.; Roberts, P. E.; Sanborn, R. H.; Tsugawa, R. T. *J. Chem. Phys.* **1979**, *70*, 1581.
(11) Souers, P. C.; Fuentes, J.; Fearon, E. M.; Roberts, P. E.; Tsugawa, R. T.; Hunt, J. L.; Poll, J. D. *J. Chem. Phys.* **1980**, *72*, 1679.
(12) Souers, P. C.; Fearon, E. M.; Roberts, P. E.; Tsugawa, R. T.; Poll, J. D.; Hunt, J. L. *Phys. Lett.* **1980**, *77A*, 277.
(13) Souers, P. C.; Fearon, E. M.; Stark, R. L.; Tsugawa, R. T.; Poll, J. D.; Hunt, J. C. *Can. J. Phys.* **1981**, *59*, 1408.
(14) Poll, J. D.; Hunt, J. L.; Souers, P. C.; Fearon, E. M.; Tsugawa, R. T.; Richardson, J. M.; Smith, G. H. *Phys. Rev. A* **1983**, *28*, 3147.
(15) Brooks, R. L.; Selen, M. A.; Hunt, J. L.; McDonald, J. R.; Poll, J. D.; Waddington, J. C. *Phys. Rev. Lett.* **1983**, *51*, 1077.
(16) Selen, M. A.; Brooks, R. L.; Hunt, J. L.; Poll, J. D.; MacDonald, J. R.; Waddington, J. C. *Nucl. Instrum. Methods Phys. Res., Sect. B* **1984**, *230*, 720.
(17) Brooks, R. L.; Hunt, J. L.; MacDonald, J. R.; Poll, J. D.; Waddington, J. C. *Can. J. Phys.* **1985**, *63*, 937.
(18) Brooks, R. L.; Bose, S. K.; Hunt, J. L.; MacDonald, J. R.; Poll, J. D.; Waddington, J. C. *Phys. Rev. B* **1985**, *32*, 2478.
(19) Miller, J. J.; Brooks, R. L.; Hunt, J. L.; Poll, J. D. *Can. J. Phys.* **1988**, *66*, 1025.
(20) Forest, J. A.; Brooks, R. L.; Hunt, J. L.; Stenum, B.; Schon, J.; Sorensen, H.; Guntler, P.; Magnotta, F.; Mapoles, E. R.; Souers, P. C.; Collins, G. W. *Phys. Rev. B* **1992**, *46*, 13820.
(21) Miller, J. J.; Brooks, R. L.; Hunt, J. L. *Can. J. Phys.* **1993**, *71*, 501.
(22) Momose, T.; Kerr, K. E.; Weliky, D. P.; Gabrys, C. M.; Dickson, R. M.; Oka, T. *J. Chem. Phys.* **1994**, *100*, 7840.
(23) Poll, J. D.; Hunt, J. L. *Can. J. Phys.* **1985**, *63*, 84.
(24) Miller, J. J.; Poll, J. D.; Hunt, J. L. *Can. J. Phys.* **1991**, *69*, 606.
(25) Bose, S. K.; Poll, J. D. *Can. J. Phys.* **1985**, *63*, 1105.
(26) Bose,S. K.; Poll, J. D. *Can. J. Phys.* **1987**, *65*, 58.
(27) Bose, S. K.; Poll, J. D. *Can. J. Phys.* **1985**, *63*, 94.
(28) Bose, S. K.; Poll, J. D. *Can. J. Phys.* **1987**, *65*, 67.
(29) Momose, T.; Weliky, D. P.; Oka, T. *J. Mol. Spectrosc.* **1992**, *153*, 760.
(30) Poll, J. D.; Hunt, J. L.; Souers, P. C.; Fearon, E. M.; Tsugawa, R. T.; Richardson, J. H.; Smith, G. H. *Phys. Rev. A* **1983**, *28*, 3147.
(31) Bhatnagar, S. S.; Allin, E. J.; Welsh, H. L. *Can. J. Phys.* **1962**, *40*, 9.
(32) Condon, E. U. *Phys. Rev.* **1932**, *41*, 759.
(33) Kerr, K. E.; Momose, T.; Weliky, D. P.; Gabrys, C. M.; Oka, T. *Phys. Rev. Lett.* **1994**, *72*, 3957.
(34) Van Kranendonk, J. *Solid Hydrogen, Theory of the Properties of Solid H_2, HD and D_2*; Plenum: New York, 1983.
(35) Okumura, M.; Yeh, L. I.; Lee, Y. T. *J. Chem. Phys.* **1985**, *83*, 3705.
(36) Okumura, M.; Yeh, L. I.; Lee, Y. T. *J. Chem. Phys.* **1988**, *88*, 79.
(37) (a) Redington, R. L.; Milligan, D. E. *J. Chem. Phys.* **1963**, *39*, 1276; (b) Suzer, S.; Andrews, L. *J. Chem. Phys.* **1988**, *88*, 916.
(38) Pimentel, G. C.; Bulanin, M. O.; Van Thiel, M. *J. Chem. Phys.* **1962**, *36*, 500.
(39) Yamaguchi, Y.; Gaw, J. F.; Schaefer, H. F., III. *J. Chem. Phys.* **1983**, *78*, 4074.
(40) Yamaguchi, Y.; Gaw, J. F.; Remington, R. B.; Schaefer, H. F., III. *J. Chem. Phys.* **1987**, *86*, 5072.
(41) For example, Gabrys, C. M.; Uy, D.; Jagod, M.-F.; Oka, T.; Amano, T. *J. Phys. Chem.* **1995**, *99*, 15611.
(42) Nosanow, L. H. *Phys. Rev.* **1966**, *146*, 120.
(43) Souers, P. C. *Hydrogen Properties for Fusion Energy*; University of California Press: Berkeley, 1985.
(44) Kiefer, J. L. *At. Data Nucl. Data Tables* **1969**, *1*, 19.
(45) Oka, T. *Molecular Ions: Spectroscopy, Structure and Chemistry*; Miller, T. A., Bondyberg, V. E., Eds.; North−Holland Pub. Co.: New York, 1983; pp 73−90.
(46) Oka, T. *Rev. Mod. Phys.* **1992**, *64*, 1141.
(47) Langevin, P. *Ann. Chim. Phys.* **1905**, *5*, 245.
(48) Miyazaki, T.; Lee, K. P. *J. Phys. Chem.* **1985**, *90*, 400.
(49) Miyazaki, T.; Iwata, N.; Fueki, K.; Hase, H. *J. Phys. Chem.* **1990**, *94*, 1702.
(50) Datz, S.; Sundström, G.; Biedermann, Ch.; Broström, L.; Danared, H.; Mannervik, S.; Mowat, J. R.; Larsson, M. *Phys. Rev. Lett.* **1995**, *74*, 896.
(51) Momose, T.; Zhang, Y.; Lindsay, C. M.; Oka, T. Unpublished work.
(52) Symons, M. C. R. *Chem. Phys. Lett.* **1995**, *247*, 607.
(53) Kumada, T.; Inagaki, H.; Nagasawa, T.; Aratono, Y.; Miyazaki, T. *Chem. Phys. Lett.* **1996**, *251*, 219.
(54) (a) Sapse, A. M.; Rayez-Meaume, M. T.; Rayez, J. C.; Massa, L. J. *Nature* **1979**, *278*, 332; (b) Rayez, J. C.; Rayez-Meaume, M. T.; Massa, L. J. *J. Chem. Phys.* **1981**, *75*, 5393.